Adaptive Interference Cancellation Using Atomic Norm Minimization and Denoising

Shuang Li, Daniel Gaydos, Payam Nayeri, *Senior Member, IEEE*, and Michael B. Wakin, *Senior Member, IEEE*

***Abstract*—The rapid increase in the number of wireless devices in modern communication networks has significantly increased the number of interference sources, which severely impacts communication reliability. Adaptive interference cancellation is rapidly becoming a necessity for modern wireless networks. For interference cancellation, a digital beamformer adaptively adjusts its weight vector using an array processing algorithm. This, in turn, shapes the radiation pattern in a manner that minimizes interference power and maximizes the desired signal power. In this letter, we propose two atomic-norm-minimization-based methods to design a weight vector that can be used to cancel interference. We present numerical and experimental studies and compare with the minimum variance distortionless response beamformer, which outputs the highest possible signal-to-interference-plus-noise ratio (SINR). We show that our approach is robust to signal corruptions arising from carrier frequency offsets. Uniquely, our algorithm extracts the offset frequencies, thus enabling interference cancellation with maximum SINR.**

***Index Terms*—Array processing, atomic norm minimization (ANM), beamforming, carrier frequency offset, interference cancellation.**

I. Introduction

ADAPTIVE beamformers consist of an antenna array and an adaptive processor. In addition to high-speed beamscanning, these systems can be used for adaptive interference cancellation and high-resolution direction finding [1]–[3]. Adaptive arrays cancel interference by placing array nulls in the direction of the interferers. In a digital beamforming (DBF) receiver, each element is connected to a preamp and then to an A/D converter. The outputs of the A/Ds are connected to a coded digital data bus. A similar process is implemented in transmit. Having digital data at each element of the array provides the means to measure the covariance matrix, which is the crux of all adaptive nulling algorithms [4]. While the high cost of these systems limited their widescale deployment in the past, ongoing improvements in semiconductor technology as well as radio communications (e.g., software defined radios) have now made DBF arrays a practical option.

Adaptive algorithms typically rely on a known pilot signal, which is compared to the received pilot signal and used to form an error vector. Algorithms minimize this error vector by optimizing the weight vector of the antenna array. Digital signals collected at the elements of the array serve as the array processor input, and as such these algorithms are very sensitive to signal corruptions. Practical implementation of DBF, thus, requires one to develop robust solutions for nonideal scenarios, commonly known as mismatched beamformers [5]–[11]. Robust algorithms have primarily focused on mismatches from steering vector (SV) errors, or finite sample size of the spatial spectral estimates. While the latter problem is outside the scope of this work, SV mismatch has some similarities, however with subtle differences [6]–[9]. SV errors arise from direction-of-arrival mismatch, or perturbed arrays with errors in element location, phase, or gain, and have shown to result in severe performance degradation. The most widely adopted solution to these problems is diagonal loading [6], [7] and equivalent approaches. These techniques provide robustness to SV errors by effectively designing for a higher white noise level than is actually present, and as such are usually practical when signal-to-interference ratio (SIR) is more important than signal-to-interference-plus-noise ratio (SINR). To mitigate some of these issues, variable loading [8], [9] has been introduced; it can improve robustness to SV errors while maintaining a desired SIR or SINR.

On the other hand, in [12], it was shown that carrier frequency offsets between the transmitter and receiver corrupt the received signal and prevent it from matching the pilot signal due to low correlation between the signals. If carrier frequency offsets can be measured and corrected before interference cancellation, this issue can be resolved. However, in high-interference and high-multipath environments, measuring the carrier frequency offset is usually not possible. In this letter, we introduce a new interference cancellation algorithm based on atomic norm minimization (ANM) that provides robustness to this type of signal corruption. While existing beamforming techniques can provide robustness to certain mismatch issues such as SV errors, and usually at the expense of a higher noise, to the best of our knowledge, no existing approach is designed to provide robustness toward signal corruptions arising from carrier frequency offsets. We present numerical and experimental results and show that our proposed approach is naturally capable of extracting the offset frequencies that cause signal corruption. As such, robustness is

Manuscript received September 29, 2020; accepted October 13, 2020. Date of publication October 21, 2020; date of current version December 22, 2020. The work of Shuang Li and Michael B. Wakin was supported by the NSF under Grant CCF-1704204. *(Corresponding author: Payam Nayeri.)*

Shuang Li was with the Electrical Engineering Department, Colorado School of Mines, Golden, CO 80401 USA. She is now with the Department of Mathematics, University of California, Los Angeles, CA 90095 USA (e-mail: shuangli@alumni.mines.edu).

Daniel Gaydos was with the Electrical Engineering Department, Colorado School of Mines, Golden, CO 80401 USA. He is now with Zeta Associates, Aurora, CO 80011 USA (e-mail: dgaydos@alumni.mines.edu).

Payam Nayeri and Michael B. Wakin are with Electrical Engineering Department, Colorado School of Mines, Golden, CO 80401 USA (e-mail: pnayeri@mines.edu; mwakin@mines.edu).

Digital Object Identifier 10.1109/LAWP.2020.3032894

achieved with maximum SINR and without any degradation to other system performance characteristics.

II. ANM for Adaptive Interference Cancellation

A. Atomic Norm Minimization

In recent years, ANM has been extensively studied in both line spectral estimation and array signal processing for localizing the off-grid temporal or angular frequencies of sinusoidal components [13]–[20]. Consider a sampled spectrally sparse signal $\boldsymbol{x} \in \mathbb{C}^M$ with K different active frequencies

$$\boldsymbol{x} = \sum_{k=1}^{K} c_k \boldsymbol{a}(f_k) \in \mathbb{C}^M \tag{1}$$

where $\boldsymbol{a}(f) \triangleq [1\, e^{j2\pi f} \cdots e^{j2\pi f(M-1)}]^\top \in \mathbb{C}^M$ is a vector[1] containing M uniform samples of a complex exponential signal with frequency $f \in [0,1)$, and the scalars c_k denote the complex coefficients. As in [13]–[20], one can define an atomic set $\mathcal{A}$ consisting of all possible such complex exponentials: $\mathcal{A} = \{\boldsymbol{a}(f) : f \in [0,1)\}$. This atomic set induces a corresponding *atomic norm* $\|\boldsymbol{x}\|_{\mathcal{A}} := \inf\{\sum_{k=1}^{K} |c_k| : \boldsymbol{x} = \sum_{k=1}^{K} c_k \boldsymbol{a}(f_k)\}$.

The atomic norm is analogous to the ℓ_1 norm commonly used in compressive sensing and sparse signal recovery with finite dictionaries, but in this case, the dictionary is the continuously parameterized atomic set $\mathcal{A}$. When solving an inverse problem with multiple candidate solutions, minimizing ℓ_1 or atomic norm will promote sparsity in the solution. In particular, note that any signal $\boldsymbol{x}$ obeying (1) can be represented with only K atoms from the atomic set $\mathcal{A}$. When $\boldsymbol{x}$ is observed with missing or noisy entries, then optimization problems that attempt to minimize the atomic norm will promote spectral sparsity and can lead to exact or approximate recovery of $\boldsymbol{x}$ [13]–[20]. Notably, this is possible even when the frequencies f_k are "off grid," i.e., not restricted to the Nyquist frequencies $0, \frac{1}{M}, \frac{2}{M}, \ldots, \frac{M-1}{M}$.

B. Problem Formulation

Consider a conventional linear array with N antenna elements. By collecting M snapshots on each element, one can formulate a data matrix

$$\mathbf{X}^\star = \sum_{k=1}^{K} (\boldsymbol{s}_k \odot \boldsymbol{a}(f_k)) \mathbf{asv}(\theta_k) \in \mathbb{C}^{M \times N} \tag{2}$$

where $\boldsymbol{s}_k$ denotes the desired signal (if $k = 1$) or interferers (if $k > 1$), and $\odot$ denotes elementwise vector multiplication. Here, we assume that the desired signal and the interferers $\{\boldsymbol{s}_k\}_{k=1}^K$ are uniformly sampled complex exponential signals, namely, $\boldsymbol{s}_k = [1\, e^{j2\pi f_k^o} \cdots e^{j2\pi f_k^o (M-1)}]^\top$ for $k = 1, \ldots, K$, where f_k^o denotes the known frequency of the desired signal (if $k = 1$) or the unknown frequency of the interferers (if $k > 1$). The modulation by the vector $\boldsymbol{a}(f_k)$ models an unknown frequency offset f_k. Finally, $\mathbf{asv}(\theta_k) \triangleq e^{j2\pi \sin(\theta_k)\boldsymbol{q}}$ denotes the array SV with $\boldsymbol{q} \in \mathbb{R}^{1\times N}$ being the element positions and θ_k being the angle to the desired source (if $k = 1$) or interferers (if $k > 1$).

Our goal, in this letter, is to design a weight vector $\boldsymbol{w} \in \mathbb{C}^N$ for an array such that the array output is $\mathbf{X}^\star \boldsymbol{w} = \boldsymbol{s}_1$ when given the data matrix $\mathbf{X}^\star$ and the desired signal $\boldsymbol{s}_1$. That is, the array output only contains the desired signal and the interferers are completely cancelled. This problem has been heavily studied in array signal processing. One of the most popular adaptive array beamformers is the minimum variance distortionless response (MVDR) beamformer, which provides noise resilience while nulling out interferers, and outputs the highest possible SINR. When the covariance matrix of interference and noise is replaced by the sample matrix obtained using a set of training (secondary) data, the adaptive version of the MVDR beamformer is referred to as the sample matrix inversion (SMI) beamformer [5], [11]. Here, we use the SMI beamformer as the reference for comparison with our proposed algorithm. SMI minimizes the mean-squared error between the beamformer output and desired signal by directly applying the pseudoinverse matrix, i.e., $\boldsymbol{w} = \mathbf{X}^{\star\dagger} \boldsymbol{s}_1$.

To remove the impact of the unknown frequency offset, we propose to design the weight vector $\boldsymbol{w}$ as

$$\boldsymbol{w} = \mathbf{X}^{\star\dagger}(\boldsymbol{s}_1 \odot \boldsymbol{a}(f_1)) \tag{3}$$

which is inspired by the SMI method. To do this, note that we need to estimate the signal frequency offset f_1 first. As described ahead, we obtain this estimate using ANM.

Define a matrix atomic set as

$$\mathcal{A}_M = \{\mathbf{A}(f^o + f, \mathbf{asv}(\theta)) : f^o + f \in [0,1), \mathbf{asv}(\theta) \in \mathbb{C}^{1\times N}\}$$

with $\mathbf{A}(f^o + f, \mathbf{asv}(\theta)) \triangleq \boldsymbol{a}(f^o + f)\mathbf{asv}(\theta)$. Observe that the data matrix in (2) can be rewritten as $\mathbf{X}^\star = \sum_{k=1}^{K} \mathbf{A}(f_k^o + f_k, \mathbf{asv}(\theta_k))$, and thus, $\mathbf{X}^\star$ can be represented with only a few atoms from the atomic set $\mathcal{A}_M$. Now, define the corresponding matrix atomic norm of an arbitrary matrix $\mathbf{X}$ as

$$\|\mathbf{X}\|_{\mathcal{A}_M} = \inf\left\{\sum_k c_k : \mathbf{X} = \sum_k c_k \mathbf{A}(f_k^o + f_k, \mathbf{asv}(\theta_k)),\ c_k \geq 0\right\}.$$

Given $\mathbf{X}^\star$, to recover $\{f_k^o + f_k\}_{k=1}^K$ and thus get f_1, we can solve the following ANM problem as in [16]–[18]:

$$\min_{\mathbf{X}} \|\mathbf{X}\|_{\mathcal{A}_M} \text{ s.t. } \mathbf{X} = \mathbf{X}^\star. \tag{4}$$

Problem (4) is equivalent to the following semidefinite program (SDP):

$$\min_{\mathbf{X},\boldsymbol{u},\mathbf{V}} \ \frac{1}{2M}\mathrm{Tr}(\mathcal{T}(\boldsymbol{u})) + \frac{1}{2}\mathrm{Tr}(\mathbf{V}) \quad \text{s.t.} \quad \begin{bmatrix} \mathcal{T}(\boldsymbol{u}) & \mathbf{X} \\ \mathbf{X}^* & \mathbf{V} \end{bmatrix} \succeq 0,\ \mathbf{X} = \mathbf{X}^\star \tag{5}$$

where $\mathcal{T}(\boldsymbol{u})$ is a Hermitian Toeplitz matrix with $\boldsymbol{u}$ as its first column, and $\mathrm{Tr}(\cdot)$ denotes the trace of a matrix. Although the primal problem (4) has a trivial solution ($\mathbf{X} = \mathbf{X}^\star$), its usefulness comes from the fact the dual solution $\mathbf{Q}$ of (4) carries information about the unknown frequencies. (The off-the-shelf SDP solver CVX [21] can return the dual solution $\mathbf{Q}$ of (4).) In particular, using $\mathbf{Q}$, one can formulate the dual polynomial $\mathcal{Q}(f) = \mathbf{Q}^* \boldsymbol{a}(f)$ and identify the frequencies $\{f_k^o + f_k\}_{k=1}^K$ by localizing the places where the dual polynomial achieves $\|\mathcal{Q}(f)\|_2 = 1$ [16, Prop. 1]. The frequency pair $f_k^o + f_k$ closest to the anticipated value f_1^o is identified as the desired frequency

[1]Note that we use superscripts $^\top$ and * to denote transpose and conjugate transpose, respectively.

plus offset and used in (3) to construct the weight vector $\boldsymbol{w}$. We refer to this method as ANM+SMI since it is inspired by both ANM and SMI.

It follows from [17, Th. 4] that $\mathbf{X}^\star = \sum_{k=1}^{K}(\boldsymbol{s}_k \odot \boldsymbol{a}(f_k))\mathbf{a}\mathbf{s}\mathbf{v}(\theta_k)$ is the unique atomic decomposition that achieves the atomic norm $\|\mathbf{X}^\star\|_{\mathcal{A}_M}$ if the minimum separation between the frequencies $\{f_k^o + f_k\}_{k=1}^K$ is $\mathcal{O}(1/M)$ and $M \geq 257$. Note that $M \geq 257$ is only a technical requirement and is not required in practice. This guarantees that the frequencies can be recovered via solving the aforementioned SDP (5) and localizing the places where the dual polynomial achieves $\|\mathcal{Q}(f)\|_2 = 1$.

In the case when the data matrix $\mathbf{X}^\star$ is contaminated by Gaussian noise, one can solve the following atomic norm denoising (AND) problem: $\min_{\mathbf{X}} \frac{1}{2}\|\mathbf{Y} - \mathbf{X}\|_F^2 + \lambda\|\mathbf{X}\|_{\mathcal{A}_M}$, where $\mathbf{Y} = \mathbf{X}^\star + \mathbf{E}$ is the observed data with $\mathbf{E}$ being the noise matrix, and λ is a regularization parameter that depends on the noise variance and dimension of the problem [18]. We refer to this method as AND+SMI. Similar to ANM+SMI, one can use CVX[2] to solve the corresponding SDP of the AND problem and obtain the dual solution $\mathbf{Q}$, formulate a dual polynomial $\mathcal{Q}(f) = \mathbf{Q}^* \boldsymbol{a}(f)$ to identify the frequencies $\{f_k^o + f_k\}_{k=1}^K$, and construct the weight vector $\boldsymbol{w}$ using the signal frequency offset f_1. As shown in [18, Th. III.6], when the entries of $\mathbf{E}$ follow $\mathcal{CN}(0, \sigma^2)$ and the minimum separation between the frequencies $\{f_k^o + f_k\}_{k=1}^K$ is $\mathcal{O}(1/M)$, the denoised data matrix $\widehat{\mathbf{X}}$ obtained from solving AND with properly chosen λ satisfies $\|\widehat{\mathbf{X}} - \mathbf{X}^\star\|_F^2 = \mathcal{O}(\sigma^2 K N \log(M))$ with probability at least $1 - \frac{1}{M^2}$.

C. Numerical Studies

Using synthetic data, we compare ANM+SMI and AND+SMI with SMI. We use a uniform linear array with half-wavelength element spacing and $N = 4$ elements, i.e., the element position vector $\boldsymbol{q} = -(N-1)d/2 : d : (N-1)d/2$ with $d = 0.5$. We consider a desired signal $e^{j2\pi f_1^o t}$ with $f_1^o = 1/8$ and two interferers $2e^{j2\pi f_2^o t}$ and $3e^{j2\pi f_3^o t}$ with $[f_2^o\ f_3^o] = [1/40\ 1/50]$. The frequency offsets are set as $[f_1\ f_2\ f_3] = [1/40\ 1/50\ 1/100]$. We set the angles to the desired signal and two interferers as $\theta_1 = 10°, \theta_2 = -20°$, and $\theta_3 = 50°$. We take $M = 100$ uniform time samples at each element and formulate the data matrix $\mathbf{X}^\star$ in the noiseless case. The dual polynomial from the proposed ANM+SMI method is shown in Fig. 1(a). With this dual polynomial, we can exactly identify the frequency offset f_1 and use it to design the weight vector. The radiation pattern (array factor) and the outputs of the digital beamformer with our ANM+SMI weight and the SMI weight are shown in Figs. 1(b) and (c). It can be seen that our weight vector can correctly separate the desired signal from the two interferers. To illustrate the effect of the minimum separation between the frequencies, we repeat the previous experiment with different separation between the frequency offsets. To simplify the experiment, we only use one interferer here. We set the desired signal and interferer frequencies as 0.1 and 0.101, respectively. The number of time samples taken at each element is set as $M = 20$. We fix $f_1 = 1/40$ and set $f_2 = f_1 + \text{FreqSep}$ with FreqSep = 0.01:0.001:0.025. We present the relative error between the desired signal and the output of the digital beamformer in Fig. 1(d). It can be seen that the relative error decreases to zero when the frequency offset separation is sufficiently large. Next, we add complex Gaussian noise with variance $\sigma^2 = 0.05$ to the data matrix $\mathbf{X}^\star$ and repeat the previous experiments. The results are presented in Fig. 2. (All parameters are the same except that in Fig. 2(d); we increase the interferer frequency to 0.11, set FreqSep = 0.005:0.005:0.05, and average over 20 trials.) It can be seen that our proposed AND+SMI method still significantly outperforms SMI.

[2]Solving an SDP via CVX can be slow when dealing with high-dimensional signals. We leave the development of fast alternatives for future work.

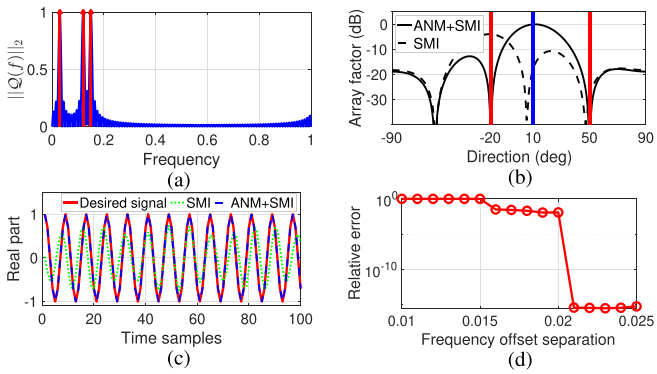

Fig. 1. Interference cancellation with ANM+SMI in the noiseless case. (a) Dual polynomial. (b) Radiation pattern (array factor). (c) Real part of the digital beamformer outputs. (d) Relative recovery error.

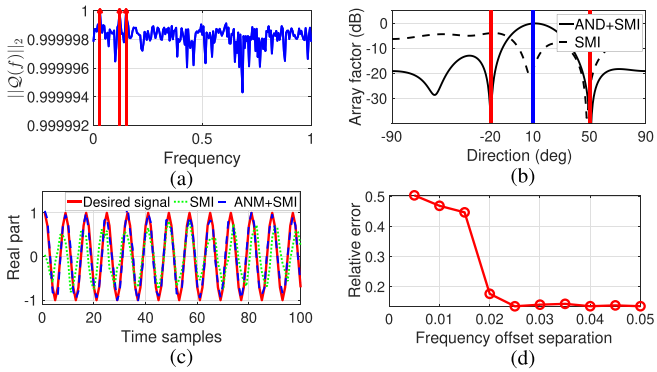

Fig. 2. Interference cancellation with AND+SMI in the noisy case. (a) Dual polynomial. (b) Radiation pattern (array factor). (c) Real part of the digital beamformer outputs. (d) Relative recovery error.

III. Experimental Results on Interference Cancellation Using a Digital Beamformer

We also test the performance of our proposed algorithm using an in-house developed digital beamformer. This beamformer is a software defined radio (SDR) array described in [12] and [21]. The hardware setup includes four National Instruments 2922 USRPs, an OctoClock-G CDA-2990 clock distribution accessory, and $N = 4$ monopole antennas. The antenna elements in the four-element linear array are spaced half-wavelengths apart and the system operates at 2.45 GHz. The OctoClock provides a trigger, which is used to synchronize all the SDRs in the array for coherent operation. In our experiments, the sample rate (after downconversion) was 500 kS/s.

In this experiment, we use two transmitters, each sending out a continuous wave (CW) signal. One signal can be viewed as

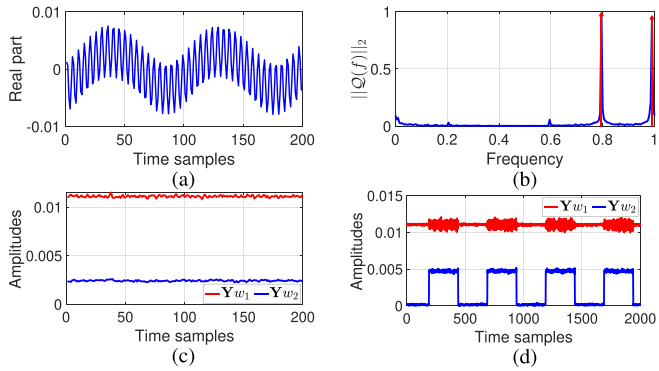

Fig. 3. Experimental interference cancellation with DBF. (a) Real part of the received signal at the first element. (b) Dual polynomial used to estimate the frequency offsets. (c) Output signals when the two transmitters send out two CW signals. (d) Output signals when one transmitter sends out a CW signal and the other sends out a square wave.

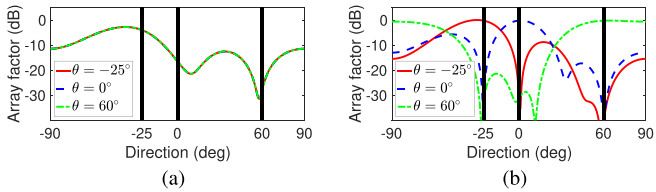

Fig. 4. Multibeam interference cancellation with DBF. (a) SMI. (b) Proposed AND+SMI method.

the desired signal and the other one as the interference. The digital beamformer is used as a receiver. We note that the transmitter is not synchronized with the receiver, meaning a carrier frequency offset exists in this setup. An example of the received signal at the first element is shown in Fig. 3(a). The received signals from all four elements can be formulated as a data matrix $\mathbf{Y}$. We can, then, apply the AND+SMI method to $\mathbf{Y}$ to estimate the frequency offsets and array weights. Note that we only use $M = 200$ time samples to compute the array weights. We also set the regularization parameter $\lambda = 1$. As shown in Fig. 3(b), one can identify the frequency offsets by localizing the peaks of $\|\mathcal{Q}(f)\|_2$. In particular, the two frequency offsets are identified as $f_1 = 0.795$ and $f_2 = 0.99$, corresponding to CW signals 102.5 kHz and 5 kHz below the receiver carrier frequency, respectively. Two weight vectors[3] $\boldsymbol{w}_1 = \mathbf{Y}^{\dagger}\boldsymbol{a}(f_1)$ and $\boldsymbol{w}_2 = \mathbf{Y}^{\dagger}\boldsymbol{a}(f_2)$ can, then, be used to separate the two transmitted signals, or equivalently, cancel the interference. We present the outputs ($\mathbf{Y}\boldsymbol{w}_1$ and $\mathbf{Y}\boldsymbol{w}_2$) of the digital beamformer in Fig. 3(c). With both weighting vectors, the beamformer output is a steady amplitude, as is consistent with a single CW signal. If both signals were present, the output would show a periodic amplitude variation resulting from the superposition of the two CW signals with different frequencies. The SINRs of the two signals are 73.14 dB and 64.00 dB for the signals at 102.5 kHz and 5 kHz below the receiver carrier frequency, respectively. SINRs were computed by removing the frequency offset from the beamformer output and projecting the result onto a constant signal to find the signal contribution to the beamformer output and, hence, the signal power. The signal was subtracted from the beamformer output to find the interference-plus-noise power. These power values were used in SINR calculations. To provide a clearer demonstration of the effectiveness of AND+SMI, we test them on another two transmitted signals, which are a CW signal and a 1 kHz square wave. (We use the same two weight vectors previously computed.) Since at 500 kS/s the square wave period is 500 samples, we kept 2000 samples at each element. Fig. 3(d) shows the outputs of the digital beamformer. It can be seen that AND+SMI again separates the two signals successfully, with one weighting vector closely recovering the CW signal and the other recovering the square wave.

[3]Note that amplitude variations in the data matrix may cause amplitude variations in the weight vectors. To address this problem, we normalized the weight vectors before performing interference cancellation.

IV. Application to Multibeam Arrays

Multibeam antenna arrays can be used to transmit or receive signals in multiple directions. Multibeam devices can be used to communicate with separate devices simultaneously, isolating communication to each device based on direction. In the case of multiple-input multiple-output systems, multibeam capability is the most effective way to increase channel capacity [22]. Generally, the choice is between analog (phased arrays) or DBF [2], [3], where the former offers the advantage of lower cost, whereas the latter offers several advantages such as wideband signal reception and transmission, large number of beams, fast beam steering, and flexibility.

In multibeam communication, each beam essentially acts as an interference source for the other beams. If for each beam, the array nulls all other channels (or beams), beam isolation can be significantly improved, which maximizes the signal-to-noise-ratio. In the following synthetic experiment, we compare AND+SMI with SMI. We consider a uniform linear array with half-wavelength element spacing and $N = 4$ elements. We consider three sources with anticipated frequencies $f^o = [1/50\ 1/50\ 1/50]$, unknown frequency offsets $f = [1/200\ 1/100\ 1/20]$, and unknown directions of arrival $\theta = [-25°\ 0°\ 60°]$. We take $M = 100$ snapshots from each sensor and add complex Gaussian noise with variance 0.05 to the clean data matrix. The resulting radiation patterns are shown in Fig. 4. It can be seen that AND+SMI outperforms SMI in its ability to isolate each source while suppressing the interference from other sources when the source frequency offsets are unknown. We note that since SMI computes the weight vector based on the anticipated frequency, which is identical for the three signals in this study, it cannot identify three separate beams and, therefore, computes a single weight vector for the array.

V. Conclusion

We propose a new adaptive interference cancellation algorithm that is robust to signal corruptions, such as carrier frequency offsets between the transmitter and receiver. Compared to other techniques, our method directly extracts the carrier frequency offsets that cause signal corruption and cancels the interference with maximum SINR. The proposed method also finds application in multibeam arrays.

REFERENCES

[1] B. Widrow, P. E. Mantey, L. J. Griffiths, and B. B. Goode, "Adaptive antenna systems," *Proc. IEEE*, vol. 55, no. 12, pp. 2143–2159, Dec. 1967.

[2] R. C. Hansen, *Phased Array Antennas*, 2nd ed., Hoboken, NJ, USA: Wiley, 2009.

[3] R. J. Mailloux, *Phased Array Antenna Handbook*, 3rd ed. Norwood, MA, USA: Artech House, 2017.

[4] H. L. Van Trees, *Optimum Array Processing: Part IV of Detection, Estimation, and Modulation Theory*. Hoboken, NJ, USA: Wiley, 2004.

[5] I. P. Gravas, Z. D. Zaharis, T. V. Yioultsis, P. I. Lazaridis, and T. D. Xenos, "Adaptive beamforming with sidelobe suppression by placing extra radiation pattern nulls," *IEEE Trans. Antennas Propag.*, vol. 67, no. 6, pp. 3853–3862, Jun. 2019.

[6] M. W. Ganz, R. L. Moses, and S. L. Wilson, "Convergence of the SMI and the diagonally loaded SMI algorithms with weak interference," *IEEE Trans. Antennas Propag.*, vol. 38, no. 3, pp. 394–399, Mar. 1990.

[7] R. L. Dilsavor and R. L. Moses, "Analysis of modified SMI method for adaptive array weight control," *IEEE Trans. Signal Process.*, vol. 41, no. 2, pp. 721–726, Feb. 1993.

[8] J. Gu, "Robust beamforming based on variable loading," *Electron. Lett.*, vol. 41, no. 2, pp. 55–56, 2005.

[9] X. Li, D.-W. Wang, X. Ma, and Z. Xiong, "Robust adaptive beamforming using iterative variable loaded sample matrix inverse," *Electron. Lett.*, vol. 54, no. 9, pp. 546–548, 2018.

[10] L. Yu, W. Liu, and R. Langley, "SINR analysis of the subtraction-based SMI beamformer," *IEEE Trans. Signal Process.*, vol. 58, no. 11, pp. 5926–5932, Nov. 2010.

[11] J. Liu, W. Liu, H. Liu, B. Chen, X.-G. Xia, and F. Dai, "Average SINR calculation of a persymmetric sample matrix inversion beamformer," *IEEE Trans. Signal Process.*, vol. 64, no. 8, pp. 2135–2145, Apr. 2016.

[12] D. Gaydos, P. Nayeri, and R. Haupt, "Adaptive beamforming in high-interference environments using a software-defined radio array," in *Proc. IEEE Int. Symp. Antennas Propag. USNC-URSI Radio Sci. Meeting*, Jul. 2019, pp. 1501–1502.

[13] V. Chandrasekaran, B. Recht, P. A. Parrilo, and A. S. Willsky, "The convex geometry of linear inverse problems," *Found. Comput. Math.*, vol. 12, no. 6, pp. 805–849, 2012.

[14] E. J. Candès and C. Fernandez-Granda, "Towards a mathematical theory of super-resolution," *Commun. Pure Appl. Math.*, vol. 67, no. 6, pp. 906–956, 2014.

[15] G. Tang, B. N. Bhaskar, P. Shah, and B. Recht, "Compressed sensing off the grid," *IEEE Trans. Inf. Theory*, vol. 59, no. 11, pp. 7465–7490, Nov. 2013.

[16] Y. Li and Y. Chi, "Off-the-grid line spectrum denoising and estimation with multiple measurement vectors," *IEEE Trans. Signal Process.*, vol. 64, no. 5, pp. 1257–1269, Mar. 2016.

[17] Z. Yang and L. Xie, "Exact joint sparse frequency recovery via optimization methods," *IEEE Trans. Signal Process.*, vol. 64, no. 19, pp. 5145–5157, Oct. 2016.

[18] S. Li, D. Yang, G. Tang, and M. B. Wakin, "Atomic norm minimization for modal analysis from random and compressed samples," *IEEE Trans. Signal Process.*, vol. 66, no. 7, pp. 1817–1831, Apr. 2018.

[19] Y. Xie, S. Li, G. Tang, and M. B. Wakin, "Radar signal demixing via convex optimization," in *Proc. 22nd Int. Conf. Digit. Signal Process.*, 2017, pp. 1–5.

[20] S. Li, M. B. Wakin, and G. Tang, "Atomic norm denoising for complex exponentials with unknown waveform modulations," *IEEE Trans. Inf. Theory*, vol. 66, no. 6, pp. 3893–3913, Jun. 2020.

[21] P. Nayeri and R. Haupt, "A testbed for adaptive beamforming with software defined radio arrays," in *Proc. IEEE/ACES Int. Conf. Wireless Inf. Technol. Syst. Appl. Comput. Electromagn.*, Mar. 2016, pp. 1–2.

[22] D. Sikri and R. M. Jayasuriya, "Multi-beam phased array with full digital beamforming for Satcom and 5G," *Microw. J.*, vol. 62, no. 4, pp. 64–79, 2019.